

# 5. Chitosan- Fe<sub>3</sub>O<sub>4</sub>Nanoparticles Cryogel for Glucose Biosensor

*by Amin Fatoni*

---

**Submission date:** 02-Feb-2023 02:09PM (UTC+0700)

**Submission ID:** 2004656746

**File name:** Fe<sub>3</sub>O<sub>4</sub>Nanoparticles\_Cryogel\_for\_Glucose\_Biosensor\_Development.pdf (4.79M)

**Word count:** 4708

**Character count:** 26246

# Chitosan-Fe<sub>3</sub>O<sub>4</sub> Nanoparticles Cryogel for Glucose Biosensor Development

Amin Fatoni<sup>1\*</sup>, Vonia Febriana Hidayah<sup>1</sup>, Suyata<sup>1</sup>, Hartiwi Diastuti<sup>1</sup>, Mekar Dwi Anggraeni<sup>2</sup>

<sup>1</sup>Department of Chemistry, Faculty of Mathematics and Natural Sciences, Universitas Jenderal Soedirman, Purwokerto, Jawa Tengah, 53122, Indonesia

<sup>2</sup>Department of Nursing, Faculty of Health Sciences, Universitas Jenderal Soedirman, Purwokerto, Jawa Tengah, 53122, Indonesia

\*Corresponding author: aminfatoni@unsoed.ac.id

## Abstract

Chitosan was widely used as a supporting material for enzyme immobilization. However, the non-conductive properties of chitosan could be a severe problem in the application of biosensors with electrochemical detection. This research aimed to modify the chitosan cryogel with Fe<sub>3</sub>O<sub>4</sub> nanoparticles for glucose biosensor application. The glucose biosensor used glucose oxidase enzyme as biological sensing element which was immobilized on the working electrode of electrochemical detection. Chitosan-Fe<sub>3</sub>O<sub>4</sub> composite cryogel was used as supporting material for glucose oxidase immobilization. The detection optimization was also performed by varying the operating conditions such as buffer pH and reaction temperature. The result showed the optimum conditions were the addition of Fe<sub>3</sub>O<sub>4</sub> nanoparticles for 4% (w/v), phosphate buffer solution of 100 mM with pH of 7.0, and reaction temperature at 25°C. The glucose determination showed linearity for increasing oxidation peak and decreasing reduction peak with the glucose concentration, with regression equation of  $y = -6.804x - 104.32$  and  $y = 4.5872x + 133.37$  respectively. Furthermore, the limit of detection and limit of quantification for oxidation peaks were 0.38 mM and 1.25 mM respectively. The reduction peak showed a limit of detection of 0.32 mM and a limit of quantification of 1.07 mM.

## Keywords

Chitosan, Cryogel, Glucose Biosensor, Nanoparticles

Received: 12 September 2022, Accepted: 16 Desember 2022

<https://doi.org/10.26554/sti.2023.8.1.52-58>

## 1. INTRODUCTION

Glucose detection methods are still challenging to develop due to the increase in diabetes mellitus cases every year. About 43% of the 3.7 million deaths are due to diabetes mellitus and mainly occur in developing countries (World Health Organization, 2016). During covid-19 pandemic, diabetes mellitus is more dangerous than the top four comorbid diseases, with 34.5% of positive confirmation covid-19 had diabetes mellitus, and 11.6% have died from covid-19 had diabetes mellitus. Furthermore, COVID-19 cases with comorbid diabetes had a 3.9-fold higher risk of death compared to those without diabetes (Wulandari et al., 2022).

The technological change encourages researchers to develop detection methods. Glucose in blood samples generally could be detected using a biosensor, where the biological sensing elements combine with a physicochemical detector. Recently, enzymatic glucose biosensors have been widely developed using glucose oxidase enzymes with electrochemical detection. Glucose oxidase immobilization on the working electrode of electrochemical detection needs a supporting material such as chitosan, albumin, or acrylamide. However, most of the polymers for enzyme immobilization are non-conductive

substances that could reduce the electron transfer of the electrochemical detection system. Several strategies have been reported to improve the conductivity of enzyme-supporting material in biosensor development, such as incorporating the multiwalled carbon nanotubes in the chitosan cryogel (Fatoni et al., 2013), polyaniline grafting to the acrylamide (Fatoni et al., 2014), nickel ferrite nanoparticles in alginate (Fatoni et al., 2021), and zinc oxide nanoparticle on the eggshell membrane (Aini et al., 2015). The use of carbon nanoparticles such as graphene and carbon nanotube provides advantages performance of glucose biosensors, however, the complex procedure of the carbon materials preparation causes relatively expensive to be applied in the biosensor market. On another side, the Fe<sub>3</sub>O<sub>4</sub> nanoparticles were easy to prepare with a low-cost materials precursor, making it more realistic to apply in the biosensor market. In this research, we develop the cryogel supporting material made of chitosan-Fe<sub>3</sub>O<sub>4</sub> nanoparticle composite for glucose biosensor supporting material. The cryogel form of enzyme-supporting materials has been reported to show several advantages such as large surface area, high sensitivity, high enzyme immobilization capacity, and ease of preparation (Fatoni et al., 2021; Samanman et al., 2015; Sezen

et al., 2021).

## 2. EXPERIMENTAL SECTION

### 2.1 Materials

Chitosan from crab shell is highly viscous, glucose oxidase from *Aspergillus niger* (type II,  $\geq 15000$  U/g solid), glutaraldehyde 25%, albumin from bovine serum (BSA), and glucose anhydrous ( $\geq 98.0\%$ ) were purchased from Sigma (Germany).  $\text{NiCl}_2 \cdot 6\text{H}_2\text{O}$ ,  $\text{FeCl}_3 \cdot 6\text{H}_2\text{O}$ , hydrogen peroxide 30%, sodium hydroxide, disodium hydrogen phosphate, and sodium dihydrogen phosphate were from Merck-milipore (Germany).

### 2.2 Apparatus and Measurements

An electrochemical study was performed using a Potentiostat (Rodeostat, IORodeo Smart Lab Technology, US) with cyclic voltammetry method, using three electrode system of graphite as working electrode, stainless steel as counter electrode and Ag/AgCl (KCl 3 M) as a reference electrode. The morphology of chitosan cryogel was observed using Scanning electron microscopy (SEM) (JSM-6510 LA, JEOL, Japan), operating at 15 kV. The nanoparticle of  $\text{Fe}_3\text{O}_4$  was observed using a transmission electron microscope (TEM).

### 2.3 $\text{Fe}_3\text{O}_4$ Nanoparticles Synthesis and Characterization

$\text{Fe}_3\text{O}_4$  nanoparticles were synthesized using the coprecipitation method (Ba-Abbad et al., 2022) by dissolving  $\text{FeSO}_4$  and  $\text{FeCl}_3$  into 30 mL of distilled water with a concentration of 1M and 2 M, respectively. The  $\text{FeSO}_4$  and  $\text{FeCl}_3$  were then mixed homogeneously and heated at  $60^\circ\text{C}$ . Then 60 mL of 0.5 M NaOH was added dropwise to the mixture, homogenized using a magnetic stirrer, and continued heating at  $80^\circ\text{C}$  for 1 hour. The nanoparticles were formed as dark brown precipitation and separated using a centrifuge. Furthermore, the obtained particles were rinsed using distilled water seven times and heated at  $90^\circ\text{C}$  for 3hr. The nanoparticles were then calcinated at  $800^\circ\text{C}$  for 1h. The obtained  $\text{Fe}_3\text{O}_4$  nanoparticles were characterized using transmission electron microscopy (TEM, JEOL JEM1400, Japan).

### 2.4 Electrode Modification

Chitosan cryogel on the working electrode has been prepared according to the previous study (Fatoni et al., 2013). Chitosan solution of 2% (w/v) was prepared in 1% (v/v) acetic acid solvent. Then the  $\text{Fe}_3\text{O}_4$  nanoparticles were added to the chitosan solution for 2 g per 100 mL chitosan solution, to obtain Chi- $\text{Fe}_3\text{O}_4$ . The Chi- $\text{Fe}_3\text{O}_4$  solution was added with 2.5% g glutaraldehyde solution as a crosslinker with a ratio of 1:100. The mixture was then dropped on the surface of the working electrode. The working electrode was then kept at  $-20^\circ\text{C}$  for 12h, continued by thawing at  $4^\circ\text{C}$  for 1h to make chitosan cryogel. The modified electrode has then tested performance using cyclic voltammetry to determine the oxidation and reduction peak of  $\text{H}_2\text{O}_2$  solution in 50 mM phosphate buffer with a pH of 7.0. The cyclic voltammetry parameters used were a potential range of -1.0 to 1.0 V and a scan rate of 0.1V/s with 5 cycles for each

measurement, performed using a potentiostat with Ag/AgCl as reference electrode and platinum wire as the counter electrode.

### 2.5 Modified Electrode Optimization

#### 2.5.1 $\text{Fe}_3\text{O}_4$ Nanoparticles Addition

This study was conducted to determine the optimal condition of the modified electrode with the addition of  $\text{Fe}_3\text{O}_4$  nanoparticles since the nanoparticle addition could increase the electron transfer, but it could increase the production cost of the biosensor. The addition of  $\text{Fe}_3\text{O}_4$  nanoparticles varied between 1; 2; 3; 4; and 5 g/100 mL of chitosan solution. The modified working electrode was tested using  $\text{H}_2\text{O}_2$  solution using the cyclic voltammetry method to observe the behavior of nanoparticle addition with increasing reduction or oxidation peaks. Optimal conditions were determined by the highest oxidation and reduction peaks to change with the lowest nanoparticles addition.

#### 2.5.2 Buffer Concentration

The modified electrode was fabricated to detect glucose using the enzyme glucose oxidase to produce an electroactive specimen of  $\text{H}_2\text{O}_2$ . The determination of  $\text{H}_2\text{O}_2$  in the solution using an electrochemical detector was facilitated by the presence of ions, therefore, the concentration of buffer solution would be greatly affecting the hydrogen peroxide determination. In this study, the phosphate buffer varied between 25; 50; 100; 150; and 200 mM as the solvent of the  $\text{H}_2\text{O}_2$  analyte. The cyclic voltammetry condition used was the same as the previous procedure. The highest oxidation or reduction peaks changes with the increased buffer concentration would be selected as the best condition of buffer concentration.

#### 2.5.3 Buffer pH

This study was conducted to determine the optimal pH of the carrier buffer which showed the modified working electrode provides the highest sensitivity. The pH test was carried out at pH 6.5; 6.75; 7; 7.25; and 7.5. The modified working electrode was tested using cyclic voltammetry to detect a 5 mM  $\text{H}_2\text{O}_2$  solution in a certain buffer concentration. The peaks of oxidation and reduction of the cyclic voltammogram were observed and a curve of the relationship between pH and the resulting current was made. Optimal conditions were shown for the buffer pH provided the highest sensitivity.

#### 2.5.4 Temperature Effect

The temperature effect was studied to determine the optimal temperature for the modified electrode provide the best condition in the hydrogen peroxide determination. The temperature behavior on the modified electrode was also crucial for enzyme catalysis in the glucose determination using immobilized glucose oxidase. Determination of the optimal temperature was performed under optimum buffer concentration and pH. Various temperatures used were 20, 25, and  $30^\circ\text{C}$  in the  $\text{H}_2\text{O}_2$  determination under optimum conditions performed using cyclic voltammetry.



## 2.6 Glucose Determination

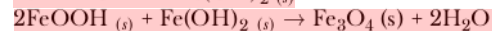
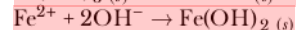
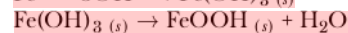
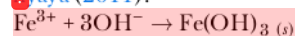
Glucose determination was performed using immobilized glucose oxidase on the modified working electrode. Glucose oxidase was dissolved in the optimum phosphate buffer pH and concentration. The chitosan-based modified electrode was then added 100  $\mu\text{l}$  of 2.5% glutaraldehyde solution and kept at room temperature for 30 min. The modified electrode was then rinsed with demineralized water to remove the excess of glutaraldehyde solution. The immobilization was performed by dropping 50  $\mu\text{l}$  glucose oxidase solution (1U/ $\mu\text{l}$ ) to the surface of the activated modified electrode and kept at 4°C for 12h. The standard glucose solution was determined using cyclic voltammetry under optimum conditions. The obtained oxidation/reduction peak with the concentration was used to calculate the linearity, limit of detection, and limit of quantification.

## 3. RESULT AND DISCUSSION

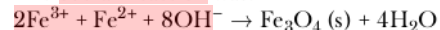
### 3.1 Fe<sub>3</sub>O<sub>4</sub> Nanoparticle Synthesis

The synthesis of Fe<sub>3</sub>O<sub>4</sub> nanoparticles in this study was carried out by the coprecipitation method using FeCl<sub>2</sub> and FeCl<sub>3</sub> precursors. The coprecipitation method is a chemical process that brings solutes down to form the desired precipitate. The most widely used iron salts to form Fe<sub>3</sub>O<sub>4</sub> nanoparticles were FeCl<sub>2</sub> and FeCl<sub>3</sub> with the precipitating compounds generally NaOH, NH<sub>4</sub>OH or in some case used tetramethyl ammonium hydroxide (TMAOH). This research used NaOH as precipitating agent. The magnetite compounds began to form at pH 9-14. Therefore, in the Fe<sub>3</sub>O<sub>4</sub> nanoparticle synthesis process, NaOH was added dropwise until it reached pH 11 at the reaction temperature of 100°C. Furthermore, the precipitate was separated, washed, and dried.

The ratio of Fe<sup>2+</sup>:Fe<sup>3+</sup> of 1:2 is intended to obtain high-purity magnetite because this ratio is stoichiometric (Mascolo et al., 2013). Several factors can determine the parameters in the synthesis of iron oxides, including iron salts, alkaline media, and temperature. The reaction for the formation of Fe<sub>3</sub>O<sub>4</sub> nanoparticles through the coprecipitation method using Fe<sup>2+</sup> and Fe<sup>3+</sup> which are reacted in an alkaline environment are as follows Laurent et al. (2008) and Ravikumar and Bandyopadhyaya (2011):



The overall reaction was:



The morphology of obtained Fe<sub>3</sub>O<sub>4</sub> nanoparticles observed using a transmission electron microscope showed a rod-like shape with length of about 40 nm and width of about 3-5 nm (Figure 1A). The rod-like shape was similar to previously reported of Fe<sub>3</sub>O<sub>4</sub> nanoparticles with great magnetic properties (Han et al., 2015). Previous studies were also reported that the Fe<sub>3</sub>O<sub>4</sub> nanoparticles produced by the coprecipitation method

ranged from 2 nm to 51 nm (Liu et al., 2006; Mürbe et al., 2008; Petcharoen and Sirivat, 2012).

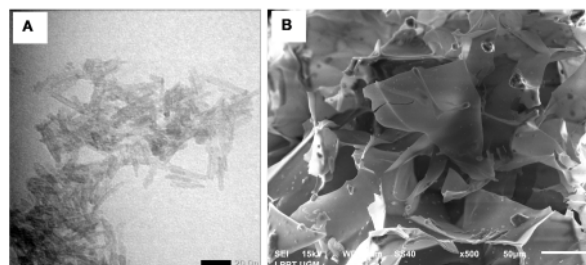


**Figure 1.** Fe<sub>3</sub>O<sub>4</sub> Nanoparticles Morphology was Observed Using a Transmission Electron Microscope (A), Chitosan-nanoparticles Cryogel was Observed Using a Scanning Electron Microscope (B)

### 3.2 Electrode Modification

Electrode surface modification used chitosan as supporting material in cryogel form (Figure 1B) for enzyme immobilization combined with Fe<sub>3</sub>O<sub>4</sub> nanoparticles as an electron transfer improver. Chitosan has been selected due to its biocompatibility, non-toxic and easy to prepare as well as maintain the enzyme activity in the biosensor development (Fatoni et al., 2013). However, chitosan showed a low electrical conductivity of  $1.91 \times 10^{-4} \mu\text{S}/\text{cm}$  (Marroquin et al., 2013), therefore, in biosensor applications using electrochemical detection, chitosan needs to be combined with conductive materials. This research used Fe<sub>3</sub>O<sub>4</sub> nanoparticles to improve chitosan conductivity, which was previously reported for electrical conductivity improvement of polyvinyl alcohol (Ramesan et al., 2018), polyaniline (Zhang et al., 2019), poly (vinylidene fluoride) (Cheng et al., 2019), and PVA-PEG-PVP blend (Hashim et al., 2018). Chitosan-Fe<sub>3</sub>O<sub>4</sub> nanoparticle composite was prepared in cryogel form for better enzyme immobilization and provided large surface area of substrate-enzyme interaction (Fatoni et al., 2013). The modified electrode using chitosan-Fe<sub>3</sub>O<sub>4</sub> nanoparticles composite in cryogel form showed a better performance of electron transfer compared to chitosan without nanoparticle or bare electrode without modification (Figure 2). The chitosan with and without nanoparticles were also different spectrum analyzed using Fourier Transform Infrared Spectroscopy (FTIR) (Figure 3). The chitosan structure contains -OH, N-H, C-H, and C-O. IR spectrum at 3448.72 cm<sup>-1</sup> showed the vibration of -OH overlapped with N-H. A weak peak at 2931.80 cm<sup>-1</sup> showed an aliphatic -CH- stretching band, and the spectrum at 1635.64 cm<sup>-1</sup> and 1257.59 cm<sup>-1</sup> showed the vibrations of the C=N group of chitosan amines. Absorption at 1095.57 cm<sup>-1</sup> indicated the presence of a C-O group of the chitosan. The presence of Fe<sub>3</sub>O<sub>4</sub> nanoparticles showed at 578.64 cm<sup>-1</sup>, which was indicated as the vibration of Fe-O typically at 560-650 cm<sup>-1</sup> (Agrin et al., 2016). The high peak at 3448.72 cm<sup>-1</sup> showed the more hydrogen bonding in

the chitosan-nanoparticles compare to the chitosan alone.

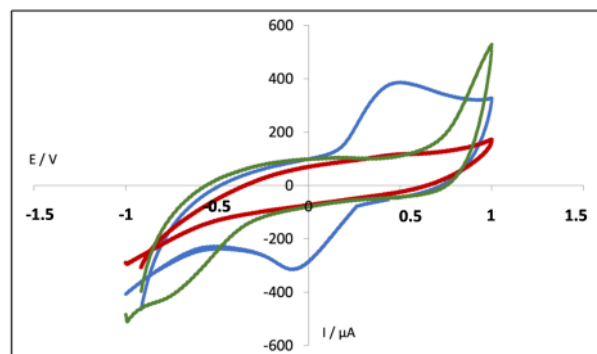


**Figure 2.** Modified Electrode (Blue) Using Chitosan- $\text{Fe}_3\text{O}_4$  Nanoparticles Composite, Chitosan Modified Electrode (Red) and Non-modified Electrode (Green) Cyclic Voltammogram Hydrogen Peroxide Determination

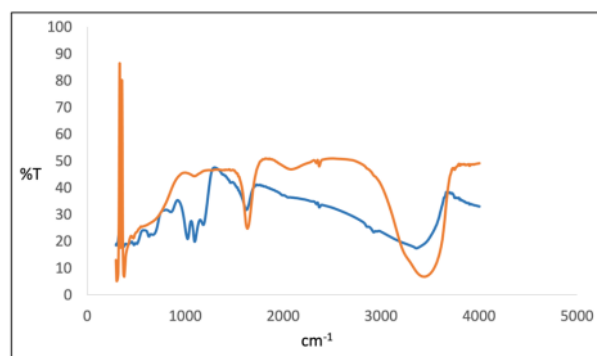


**Figure 3.** The FTIR Spectrum of Chitosan (Blue Line) and Chitosan- $\text{Fe}_3\text{O}_4$  Nanoparticle Composite (Red Line)

### 3.3 Modified Electrode Optimization

#### 3.3.1 $\text{Fe}_3\text{O}_4$ Nanoparticles Addition

$\text{Fe}_3\text{O}_4$  nanoparticles are one of the phases of iron oxide which is amphoteric and showed a homogenously spherical shape with the particle size of 10-18 nm (Koesnarpadi et al., 2015). Other properties of  $\text{Fe}_3\text{O}_4$  nanoparticles are high surface energy, low toxicity, biocompatible material, superparamagnetic behavior, high absorption capacity and the ability to transfer electrons (Ganapathe et al., 2020). Therefore, the addition of  $\text{Fe}_3\text{O}_4$  nanoparticles on the chitosan for working electrode modification could increase the sensitivity in the detection of redox reactions. However, excess  $\text{Fe}_3\text{O}_4$  nanoparticles would also be costly in biosensor fabrication. The optimum amount of  $\text{Fe}_3\text{O}_4$  nanoparticles addition should be studied in according to get the best modification formula. The results of the optimization analysis of the addition of  $\text{Fe}_3\text{O}_4$  nanoparticles can

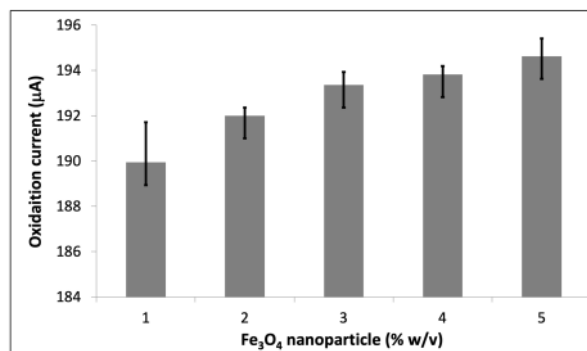


**Figure 4.** The Effect of Nanoparticles Addition on the Performance of the Modified Electrode

be seen in Figure 4. Increasing the number of nanoparticles from 1% to 3% showed an increasing oxidation current peak, however, the further addition of nanoparticles of 4% and 5% did not showed a significant increasing of the oxidation peak currents. Therefore, the best composition of chitosan composite was the addition of 3% (3g/100mL chitosan). The first nanoparticle addition showed increasing number of electron transfer, however, the excess of nanoparticles did not show a significant increasing the electron transfer due to the limitation of the working electrode surface area.

#### 3.3.2 Buffer Optimization

Buffer concentration is one of the most critical factors that can affect the sensitivity of biosensors, especially biosensors using electrochemical detection. The redox reaction of the electrochemical cell needs ions in the medium for electron transfers between the electrodes. Buffer concentration was related to the amount of ion both hydrogen as cations and hydroxy as anions, whereas the buffer pH was related to the proportion of the anion and cation in the medium. In another side, the buffer concentration and pH would also effects enzyme activity by supporting the appropriate ionic condition for the best enzyme three-dimensional structure. Therefore, the change in buffer concentration could affect the enzyme activity as well as biosensor sensitivity.

The result showed oxidation current increased with the addition of buffer concentration of 25 mM to 10 mM and then decreased afterward (Figure 5), therefore, the amount of the appropriate ions in the medium for hydrogen peroxide was best on the concentration of buffer of 100 mM. The ions in the electrochemical medium consist of cations and anions. The acidic pH provides more cations compared to the alkaline pH medium in the electrochemical detection. The results showed that increasing pH from 6.5 to 7.0 increase the oxidation current peaks, whereas the further increasing pH of 7.0 to 7.5 slightly decreases the oxidation current of hydrogen peroxide determination (Figure 6). The electrochemical detection of the analyte required the fit condition between the amount of

the ions, represented by the concentration of the buffer and the type of ions represented by the buffer pH. Therefore, the pH of 7.0 was the best condition for the modified electrode to detect hydrogen peroxide.

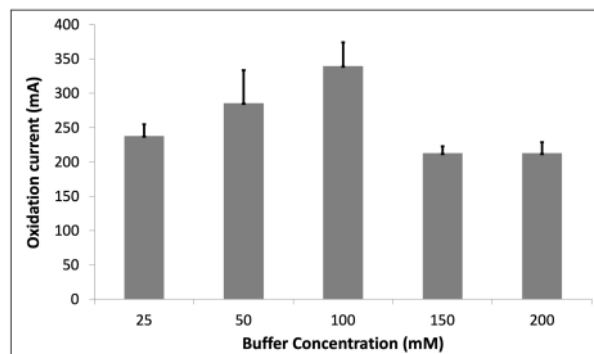


**Figure 5.** Effect of Buffer Concentration on the Modified Electrode Performance to Detect Hydrogen Peroxide Using Cyclic Voltammetry

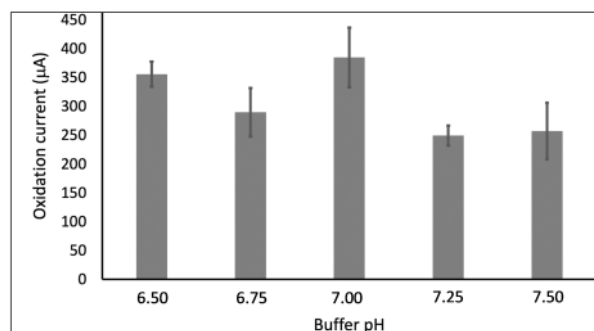


**Figure 6.** Effect of Buffer pH on the Modified Electrode Performance to Detect Hydrogen Peroxide

### 3.3.3 Temperature Effect

Temperature in the reaction related to the energy of the species such as ions in the electrochemical cell. Increasing temperature resulted in a higher energy of the electrolyte therefore resulting different behavior of redox potential in the cyclic voltammogram. The increasing temperature would also increase the mobility of ions, related to the oxidation – reduction peak height in the CV. However, the electrochemical detection in the biosensor where enzyme used as biological sensing element, the high temperature reaction could disturb the three-dimensional structure of the protein and decrease the enzyme activity. In this research, the temperature of 20 to 30°C were observed on the modified electrode for hydrogen peroxide determination. The result showed an increasing temperature of 20°C to 25°C would also increase the oxidation peak, whereas

the higher temperature of 30°C showed the decreasing of the oxidation peak (Figure 7). Increasing temperatures from 20°C to 25°C resulted in higher molecular collision between reactant resulted in higher reaction product, showed in the higher response of the modified electrode. Therefore, 25°C was the best temperature for the modified electrode on the hydrogen peroxide determination.

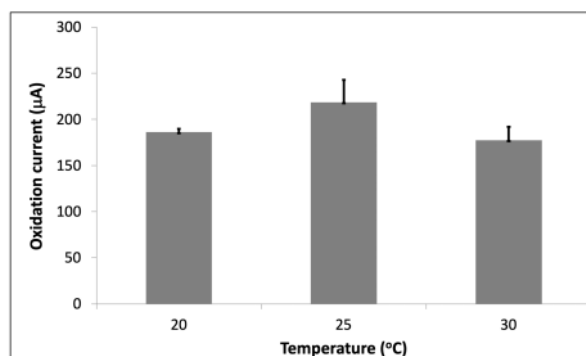


**Figure 7.** Effect of Temperature on the Modified Electrode Performance for Hydrogen Peroxide Determination

### 3.3.4 Glucose Determination

The modified electrode using chitosan- $\text{Fe}_3\text{O}_4$  nanoparticle composite cryogel as supporting material uses glucose oxidase enzyme for glucose biosensing element. The glucose oxidase was immobilized using glutaraldehyde which allow binding the amine group of chitosan in one side and amine group of glucose oxidase in another side. The composition, buffer and temperature used was the optimum condition in the previous optimization steps. The result showed the oxidation peak increased with the increase of glucose concentration (Figure 8a). The oxidation peaks of the glucose determination using the fabricated biosensor showed at about 0.25 V and reduction peaks of about -0.3 V against Ag/AgCl reference electrode. The main advantage of the fabricated glucose biosensor was used low applied potential for both reduction and oxidation peaks. The low applied potential could avoid the common interference of ascorbic acid and uric acid. This low applied potential was better than previously reported glucose biosensor using chitosan as supporting material such as graphene oxide-cobalt-Chitosan at 0.6V (Kim et al., 2022), chitosan-Au-Ti nanoparticles at 0.8V (Lipińska et al., 2021), chitosan-gold nanoparticle at 0.7V (Luo et al., 2004) and chitosan-functionalized graphene at 0.3V (Zou et al., 2019). Furthermore, both the oxidation and reduction peaks showed linear responses with regression equation of  $y = 4.5872x + 133.37$  for oxidation peaks (Figure 8b) and  $y = -0.804x - 104.32$  for reduction peaks (Figure 8c). Furthermore, the limit of detection and limit of quantification have been calculated using the obtained regression equation. For glucose detection based on the oxidation potential, the calculated LOD and LOQ were 0.32 mM and 1.07 respectively.



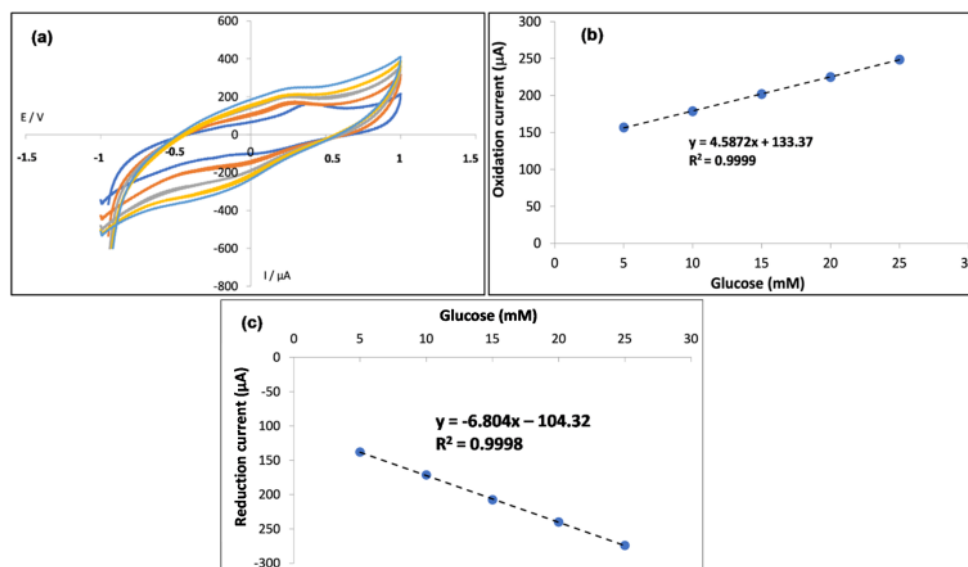


**Figure 8.** Glucose Determination Using the Fabricated Biosensor Showed Oxidation and Reduction Peaks (a) with a Linear Response for Both Oxidation (b) and Reduction (c) of Standard Glucose Solution from 5 mM to 25 mM

Whereas for the reduction potential-based glucose determination, the calculated LOD and LOQ were 0.38 mM and 1.25 mM, respectively.

#### 4. CONCLUSION

The glucose biosensor has been fabricated using glucose oxidase enzyme and chitosan- $\text{Fe}_3\text{O}_4$  nanoparticles cryogel as supporting material for enzyme immobilization. The best condition for the chitosan-nanoparticles composite was  $\text{Fe}_3\text{O}_4$  nanoparticles addition of 4% (w/v). The optimum condition for glucose biosensor measurements were buffer pH of 7.0, buffer concentration of 100 mM and reaction temperature of 25°C. Under the optimum condition, the glucose biosensor showed liner responses of  $y = -6.804x - 104.32$  and  $R^2$  of 0.999 for reduction potential and regression equation of  $y = 4.5872x + 133.37$  dan  $R^2$  of 0.999 for oxidation potential.

#### 5. ACKNOWLEDGMENT

We would like to thank the Universitas Jenderal Soedirman, Indonesia Research Grant of "Riset Unggulan Perguruan Tinggi" contract number of T/533/UN23.18/PT.01.03/2022.

#### REFERENCES

- Agrin, F. P., Z. L. Wildan, T. Grace, H. Ari, M. Mujamilah, and A. Budi (2016). Sintesis dan Pencirian Nanopartikel  $\text{Fe}_3\text{O}_4$  dalam Hidrogel Kitosan. *Majalah Polimer Indonesia*, 19(1); 23-39 (in Indonesia)
- Aini, B. N., S. Siddiquee, K. Ampon, K. F. Rodrigues, and S. Suryani (2015). Development of Glucose Biosensor

Based on ZnO Nanoparticles Film and Glucose Oxidase-immobilized Eggshell Membrane. *Sensing and Bio-Sensing Research*, 4; 46-56

- Ba-Abbad, M. M., A. Benamour, D. Ewis, A. W. Mohammad, and E. Mahmoudi (2022). Synthesis of  $\text{Fe}_3\text{O}_4$  Nanoparticles with Different Shapes Through a Co-Precipitation Method and Their Application. *JOM*, 74(9); 3531-3539
- Cheng, H., S. Wei, Y. Ji, J. Zhai, X. Zhang, J. Chen, and C. Shen (2019). Synergetic Effect of  $\text{Fe}_3\text{O}_4$  Nanoparticles and Carbon on Flexible Poly (Vinylidene Fluoride) Based Films with Higher Heat Dissipation to Improve Electromagnetic Shielding. *Composites Part A: Applied Science and Manufacturing*, 121; 139-148
- Fatoni, A., A. Numnuam, P. Kanatharana, W. Limbut, C. Thammakhet, and P. Thavarungkul (2013). A Highly Stable Oxygen-independent Glucose Biosensor Based on a Chitosan-albumin Cryogel Incorporated with Carbon Nanotubes and Ferrocene. *Sensors and Actuators B: Chemical*, 185; 725-734
- Fatoni, A., A. Numnuam, P. Kanatharana, W. Limbut, and P. Thavarungkul (2014). A Novel Molecularly Imprinted Chitosan-acrylamide, Graphene, Ferrocene Composite Cryogel Biosensor used to Detect Microalbumin. *Analyst*, 139(23); 6160-6167
- Fatoni, A., A. Wijonarko, M. D. Anggraeni, D. Hermawan, and H. Diastuti (2021). Alginate  $\text{NiFe}_2\text{O}_4$  Nanoparticles Cryogel for Electrochemical Glucose Biosensor Development. *Gels*, 7(4); 272
- Ganapathe, L. S., M. A. Mohamed, R. Mohamad Yunus, and D. D. Berhanuddin (2020). Magnetite ( $\text{Fe}_3\text{O}_4$ ) Nanoparti-

- cles in Biomedical Application: From Synthesis to Surface Functionalisation. *Magnetochemistry*, **6**(4); 68
- Han, C., J. Ma, H. Wu, and K. Hu (2015). A Low-cost and High-yield Production of Magnetite Nanorods with High Saturation Magnetization. *Journal of the Chilean Chemical Society*, **60**(1); 2799–2802
- Hashim, A., I. R. Agool, and K. J. Kadhim (2018). Novel of (Polymer Blend- $\text{Fe}_3\text{O}_4$ ) Magnetic Nanocomposites: Preparation and Characterization for Thermal Energy Storage and Release, Gamma Ray Shielding, Antibacterial Activity and Humidity Sensors Applications. *Journal of Materials Science: Materials in Electronics*, **29**(12); 10369–10394
- Kim, D. S., X. Yang, J. H. Lee, H. Y. Yoo, C. Park, S. W. Kim, and J. Lee (2022). Development of GO/Co/Chitosan-Based Nano-Biosensor for Real-Time Detection of D-Glucose. *Biosensors*, **12**(7); 464
- Koesnarpadi, S., S. J. Santosa, D. Siswanta, and B. Rusdianto (2015). Synthesis and Characterization of Magnetite Nanoparticle Coated Humic Acid ( $\text{Fe}_3\text{O}_4/\text{HA}$ ). *Procedia Environmental Sciences*, **30**; 103–108
- Laurent, S., D. Forge, M. Port, A. Roch, C. Robic, L. Vander Elst, and R. N. Muller (2008). Magnetic Iron Oxide Nanoparticles: Synthesis, Stabilization, Vectorization, Physicochemical Characterizations, and Biological Applications. *Chemical Reviews*, **108**(6); 2064–2110
- Lipińska, W., K. Siuzdak, J. Karczewski, A. Dolęga, and K. Grochowska (2021). Electrochemical Glucose Sensor Based on the Glucose Oxidase Entrapped in Chitosan Immobilized onto Laser-processed Au-Ti Electrode. *Sensors and Actuators B: Chemical*, **330**; 129409
- Liu, X., M. D. Kaminski, Y. Guan, H. Chen, H. Liu, and A. J. Rosengart (2006). Preparation and Characterization of Hydrophobic Superparamagnetic Magnetite Gel. *Journal of Magnetism and Magnetic Materials*, **306**(2); 248–253
- Luo, X. L., J. J. Xu, Y. Du, and H. Y. Chen (2004). A Glucose Biosensor Based on Chitosan-glucose Oxidase-gold Nanoparticles Biocomposite Formed by One-step Electrodeposition. *Analytical Biochemistry*, **334**(2); 284–289
- Marroquin, J. B., K. Y. Rhee, and S. J. Park (2013). Chitosan Nanocomposite Films: Enhanced Electrical Conductivity, Thermal Stability, and Mechanical Properties. *Carbohydrate Polymers*, **92**(2); 1783–1791
- Mascolo, M. C., Y. Pei, and T. A. Ring (2013). Room Temperature Co-precipitation Synthesis of Magnetite Nanoparticles in a Large pH Window with Different Bases. *Materials*, **6**(12); 5549–5567
- Mürbe, J., A. Rechtenbach, and J. Töpfer (2008). Synthesis and Physical Characterization of Magnetite Nanoparticles for Biomedical Applications. *Materials Chemistry and Physics*, **110**(2-3); 426–433
- Petcharoen, K. and A. Sirivat (2012). Synthesis and Characterization of Magnetite Nanoparticles via the Chemical Co-precipitation Method. *Materials Science and Engineering: B*, **177**(5); 421–427
- Ramesan, M., P. Jayakrishnan, T. Manojkumar, and G. Mathew (2018). Structural, Mechanical and Electrical Properties Biopolymer Blend Nanocomposites Derived from Poly (Vinyl Alcohol)/Cashew Gum/Magnetite. *Materials Research Express*, **5**(1); 015308
- Ravikumar, C. and R. Bandyopadhyaya (2011). Mechanistic Study on Magnetite Nanoparticle Formation by Thermal Decomposition and Coprecipitation Routes. *The Journal of Physical Chemistry C*, **115**(5); 1380–1387
- Samanman, S., A. Numnuam, W. Limbut, P. Kanatharana, and P. Thavarungkul (2015). Highly-sensitive Label-free Electrochemical Carcinoembryonic Antigen Immunosensor Based on a Novel Au Nanoparticles-graphene-chitosan Nanocomposite Cryogel Electrode. *Analytica Chimica Acta*, **853**; 521–532
- Sezen, S., V. K. Thakur, and M. M. Ozmen (2021). Highly Effective Covalently Crosslinked Composite Alginate Cryogels for Cationic Dye Removal. *Gels*, **7**(4); 178
- World Health Organization (2016). *Global Report on Diabetes: Executive Summary*. World Health Organization, Geneva
- Wulandari, E. W., S. Rotnoatmodjo, and N. Salama (2022). Diabetes Mellitus and Mortality among COVID-19 Patients in Jakarta, March–August 2020. *Kesmas: Jurnal Kesehatan Masyarakat Nasional (National Public Health Journal)*, **17**(2); 157–164
- Zhang, D., H. Chen, and R. Hong (2019). Preparation and Conductive and Electromagnetic Properties of  $\text{Fe}_3\text{O}_4/\text{PANI}$  Nanocomposite via Reverse in Situ Polymerization. *Journal of Nanomaterials*, **2019**; 7962754
- Zou, R., S. Shan, L. Huang, Z. Chen, T. Lawson, M. Lin, L. Yan, and Y. Liu (2019). High-performance Intraocular Biosensors from Chitosan-functionalized Nitrogen-containing Graphene for the Detection of Glucose. *ACS Biomaterials Science and Engineering*, **6**(1); 673–679



# 5. Chitosan-Fe<sub>3</sub>O<sub>4</sub>Nanoparticles Cryogel for Glucose Biosensor

ORIGINALITY REPORT

17%  
SIMILARITY INDEX

13%  
INTERNET SOURCES

11%  
PUBLICATIONS

6%  
STUDENT PAPERS

MATCH ALL SOURCES (ONLY SELECTED SOURCE PRINTED)

7%  
★ www.mdpi.com  
Internet Source

Exclude quotes      Off  
Exclude bibliography      On

Exclude matches      Off